*American Mineralogist, Volume 76, pages 1018–1032, 1991*

# Observations of the $\alpha$-$\beta$ phase transition in quartz: A review of imaging and diffraction studies and some new results

PETER J. HEANEY,* DAVID R. VEBLEN
Department of Earth and Planetary Sciences, The Johns Hopkins University, Baltimore, Maryland 21218, U.S.A.

## ABSTRACT

Although the $\alpha$-$\beta$ quartz transition traditionally has been treated as a simple, second-order phase transition, a wealth of studies performed over the past two decades has documented the complex nature of this transformation. It now appears that $\alpha$ quartz undergoes a first-order transition to an incommensurately modulated phase that is stable over a 1.3 °C interval. This intermediate phase consists of an ordered mosaic of Dauphiné microtwins that occur as triangular prisms elongate along c, and these prisms grow finer with increasing temperature. The discovery of this incommensurate phase was achieved through a series of diffraction and imaging experiments using a variety of methods, and this paper reviews the process by which the existence of the intermediate phase of quartz was established.

In addition, we present results from our own transmission electron microscopy experiments on the $\alpha$-$\beta$ transition. Specifically, we have determined that the sizes of the Dauphiné twins as imaged in real space are identical to the structural superperiodicities inferred from satellite reflections obtained by electron diffraction of the intermediate phase; this result supports the microtwin model presented by Van Tendeloo et al. (1976) rather than the configuration wave model of Gouhara and Kato (1985a, 1985b). Further, our observation of diffuse satellite intensities surrounding the primary Bragg peaks of $\beta$ quartz suggests that the $\beta$ polymorph has a dynamic structure in which oscillating tetrahedra are correlated over short distances.

## INTRODUCTION

The inference that room-temperature quartz transforms to a distinct polymorph upon heating first was made by Le Chatelier in 1889 based upon thermal expansion experiments. With the determination of the structural relationship between $\alpha$ and $\beta$ quartz through X-ray diffraction studies (Gibbs, 1925; Bragg and Gibbs, 1925), it was realized that the transition from one phase to the other involves only the bending, not the breaking, of primary bonds. In fact, despite some early studies that detected a discontinuity in the molar enthalpy of the transition (Perrier and Roux, 1923; Bates and Phelps, 1927), the $\alpha$-$\beta$ quartz transformation commonly has been regarded as the classic example of a second-order, displacive phase transition, as defined by Buerger (1951).

Within the past two decades, however, researchers have demonstrated that an incommensurate phase separates the $\alpha$ and $\beta$ stability fields. The transition from $\alpha$ quartz to this modulated phase appears to be a first-order one, whereas the subsequent transition from the intermediate to the $\beta$ phase probably is second order. If some geologists are not aware of the detailed transition behavior of quartz, it may be attributed to the fact that nearly all of the recent research on this transformation has been performed by scientists working in Europe and in Japan, and most of this work has been published in the physics literature.

Nevertheless, the implications of these studies are particularly important to mineral physicists and to those who would model petrologic systems thermodynamically. This article reviews the structural changes involved in the $\alpha$-$\beta$ quartz transition as determined by a multitude of imaging and diffraction techniques. Although the results of several spectroscopic experiments are invoked to clarify the dynamic processes attending the transition, a report of all the spectroscopic work on the transformation would require a separate paper. Some of the major contributions outside of diffraction studies include the following: Raman and infrared spectroscopy (Raman and Nedungadi, 1940; Saksena and Narain, 1949; Krishnamurti, 1958; Kleinman and Spitzer, 1962; Shapiro and Cummins, 1968); Brillouin spectroscopy (Shapiro and Cummins, 1968; Berge et al., 1984); inelastic neutron scattering (Axe and Shirane, 1970; Boysen et al., 1980); light scattering (Yakovlev et al., 1956; Dolino, 1980; Shigenari and Shionoya, 1985); and thermal analyses (Keith and Tuttle, 1952; Ghiorso et al., 1979; Zeyen et al., 1983; Hatta et al., 1985). Dolino (1990) offers a highly readable review

* Present address: Department of Earth Sciences, University of Cambridge, Downing Street, Cambridge CB2 3EQ, United Kingdom.

0003–004X/91/0506–1018$02.00

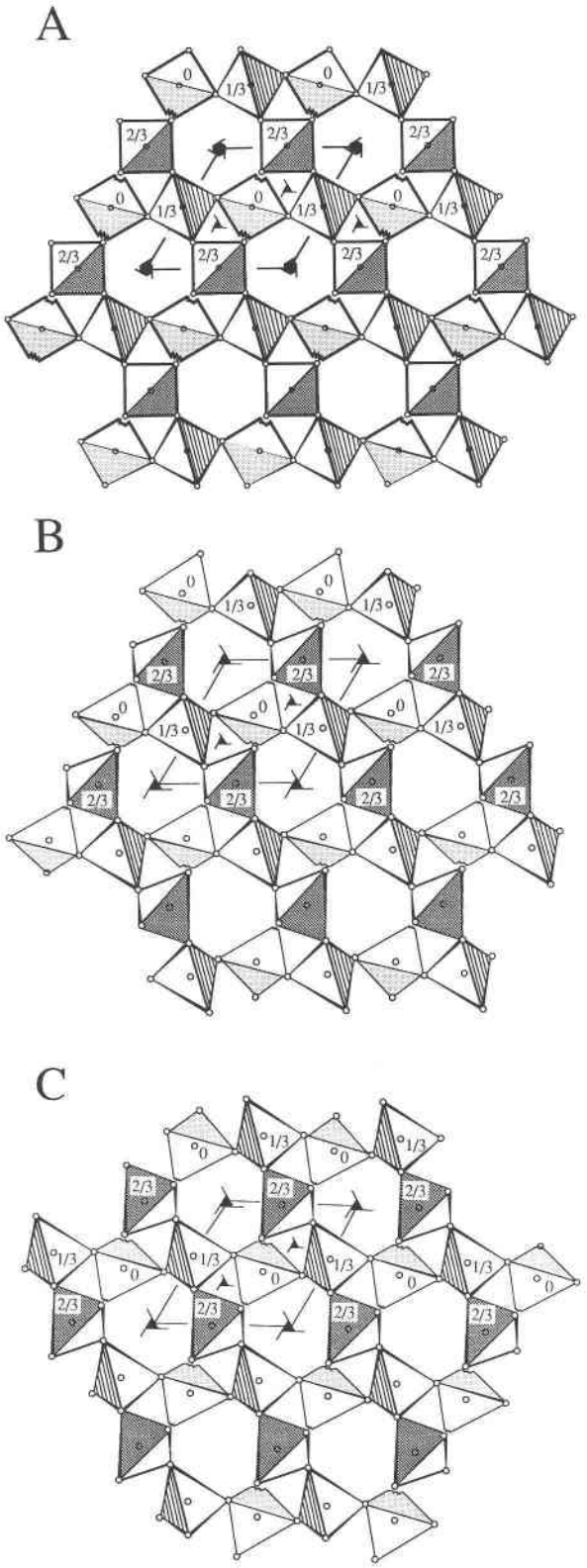


Fig. 1. (**A**) The structure of $\beta$ quartz projected down the c-axis. (**B**), (**C**) Projections of the two Dauphiné twin orientations of $\alpha$ quartz down the c-axis. Note that the two structures are related by a 180° rotation around c. (After Papike, 1988.)

of both spectroscopic studies of the $\alpha$-$\beta$ quartz transition and of applications of Landau transition theory to this transformation.

In addition to the overview of work done by others, this article will include some of the results of our own in situ heating experiments on the $\alpha$-$\beta$ phase transition using the transmission electron microscope (TEM).

## Crystallography

### Structure of $\alpha$ and $\beta$ quartz

In $\beta$ quartz, paired helical chains of silica tetrahedra spiral, in the same sense, around $6_4$ or $6_2$ screw axes parallel to **c**, and they interconnect via bridging tetrahedra, which are themselves members of adjacent helices (Fig. 1A). The two chains within each helix are symmetrically related to each other by the twofold axis contained within the sixfold screw axes, and the space group of the structure is $P6_422$ (or $P6_222$). When $\beta$ quartz is cooled below approximately 573 °C, however, the tetrahedral chains kink such that they are no longer related by the twofold rotation around **c** (Figs. 1B, 1C), and this symmetry loss causes the space group to degenerate to the subgroup $P3_121$ (or $P3_221$).

Although the chirality of the $\beta$ structure obviously is retained in the lower-temperature $\alpha$ polymorph, the down-temperature transition does produce twins. As described by Megaw (1973) and Grimm and Dorner (1975), the conversion of $\beta$ to $\alpha$ quartz can be described geometrically by rotating rigid tetrahedra around the $\langle 100 \rangle$ axes through an angle $\theta$ (see Fig. 2); in the $\beta$ structure $\theta$ is zero, but in $\alpha$ quartz at room temperature, $\theta$ is either positive or negative 16.3°. The two possible directions of tetrahedral tilt are equally likely, and they give rise to two distinct $\alpha_1$ and $\alpha_2$ twin orientations, commonly denoted as Dauphiné twins. As can be seen readily from the projections of the ditrigonal tunnels in Figures 1B and 1C, one Dauphiné twin can be transformed to the other by a 180° rotation around **c**; thus, as expected, the twin orientations are related by the twofold axis lost during the transformation.

From this model it also can be seen that the structure of $\beta$ quartz can be described geometrically as a spatial average of the two Dauphiné twin configurations. Furthermore, it is clear that the $\alpha_1$ orientation can be converted to the $\alpha_2$ by rotating individual silica tetrahedra 33° around the $\langle 100 \rangle$ axes in the proper directions. Such an operation at room temperature would entail a minor displacement of the Si atoms (approximately 0.34 Å) and a somewhat larger movement of the O atoms (approximately 0.81 Å). If these tetrahedra were to oscillate from one orientation to the other at extremely high frequencies, the resulting structure would be symmetrically indistinguishable from the static structure of ideal hexagonal $\beta$ quartz, pictured in Figure 1A.

This realization has raised the prospect that the high-temperature $\beta$ polymorph is not a static structure, in which each atom occupies a single equilibrium position, but that

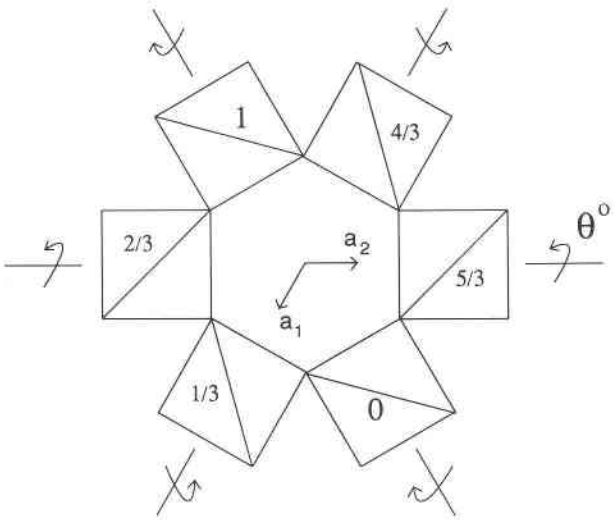


Fig. 2. A projection of a single spiraling tetrahedral chain down **c** of the ideal hexagonal $\beta$ structure. The Dauphiné twin orientation of Figure 1B can be produced by rotating individual tetrahedra in the senses indicated about the ⟨100⟩ directions. Rotation in the opposite sense results in the Dauphiné orientation of Figure 1C.

$\beta$ quartz is a dynamic structure, with each atom librating between two potential minima; $\beta$ quartz then would be a temporal average and not merely a spatial average of the two $\alpha$ orientations. In addition, the transition from $\beta$ to $\alpha$ quartz might be perceived as an ordering event, in which the initially random motions of fluctuating tetrahedra begin to correlate over macroscopic distances as $T_c$ is approached from higher temperatures, until the tetrahedra lock into one of the Dauphiné orientations at the critical temperature itself.

## Experimental procedures

Our experiments were performed on samples cut from a transparent, doubly terminated quartz crystal from Hot Springs, Arkansas (U.S. National Museum no. R17684-2). Specimens were sectioned normal to the morphological **c**, **a**, and [120] axes at a thickness of ~30 $\mu$m and thinned further by Ar ion milling. Unsupported foils of 3 mm diameter were then coated lightly with amorphous C.

Electron microscopy was performed with a Philips 420 microscope equipped with T or ST objective lenses and operated at 120 keV. Heating experiments were carried out with a Gatan Model 628 single-tilt heating holder. Specimens were heated by an annular Ta furnace, which warmed in response to increases in electrical current through a Mo strip heater. Furnace temperatures were registered by a Pt-13% Rh thermocouple spot welded to the furnace body. However, the difference between the temperature of the furnace and the thin edge of the foil typically exceeded 50 °C. Coating the quartz wafers with Cu to improve heat condition did not significantly decrease the temperature differential. The furnace was heated to the quartz transition temperature at a rate of about 5 °C/min and allowed to stabilize for 1 h before experiments were begun.

X-ray analyses in the TEM were obtained with an EDAX energy-dispersive spectrometer (EDS) and a Princeton Gamma-Tech System IV analyzer, and no elements other than Si were detected.

## Imaging Dauphiné twins with X-rays and electrons

Because the two Dauphiné twin orientations are merohedral, they cannot be observed by conventional transmission light microscopy. They can be seen by reflected light in samples that have been etched with hydrofluoric acid, since the etching rate is dependent on the orientation of the **a** axes (Parrish and Gordon, 1945). However, the resolution of this technique is limited, and etching reveals only surficial twin configurations. Consequently, techniques that reveal structural information over crystal volumes have proved considerably more useful, and these techniques typically are based on differences in the way the two Dauphiné twin orientations diffract X-rays and electrons.

In selected area diffraction patterns taken from adjacent Dauphiné twins, an $hkl$ diffraction spot of one twin domain will overlie the $hk\bar{l}$ spot of the other. Dark-field images produced from a set of superimposed diffracted beams will reveal the Dauphiné twins when the constituent beams from different twin domains either are out of phase or have markedly different intensities. Lang (1965) was the first to demonstrate this principle through transmission X-ray topography of quartz plates that were 1 mm thick. In images formed from superimposed diffraction spots with disparate structure factors, such as the 301 and the $30\bar{1}$ beams, those twin domains that are diffracting strongly appear bright, whereas the weakly diffracting domains are dark. Likewise, McLaren and Phakey (1969) observed the two twin orientations at even higher resolution using TEM, and they offer a thorough analysis of the contrast obtained at Dauphiné twin domain boundaries using a variety of diffracted beams.

As revealed by these imaging techniques, the Dauphiné twin domains appear strikingly euhedral (Fig. 3). A theoretical analysis of the twin boundaries (Walker, 1983; Walker and Gooding, 1985) indicates that the trigonal symmetry of $\alpha$-quartz forces the boundary walls to be parallel to **c** and limits the angles of the boundary wall intersections to four values: $2\epsilon°$, 60°, 120 − $2\epsilon°$, and 120 + $2\epsilon°$, where $\epsilon$ is the angle between the boundary wall and **a**. Van Landuyt et al. (1985) note that of these possibilities, $2\epsilon°$ and 60° are never observed, presumably because the excess free energy at the boundaries is positive and small angles will give rise to an increase in the boundary wall area. The two angles they do discern from their micrographs are 101° and 139°, which are consistent with our own measurements and give a value for $\epsilon$ of 9.5° near

$T_c$. Yamamoto et al. (1988) note that this angle decreases to 3° at room temperature.

McLaren and Phakey (1969) argue that the $\alpha_1$ and the $\alpha_2$ orientations can accommodate each other at the domain walls through reasonable distortions of their structures such that no breakage of bonds is necessary. A more detailed version of this model (Liebau and Böhm, 1982) suggests that as the boundary is crossed, the angle $\theta$ of tetrahedral rotation varies continuously from $-16°$ in one twin domain to $+16°$ in the other. Thus, at the center of the domain wall, the tetrahedral tilt is 0° and the structure assumes the ideal $\beta$ quartz configuration. Since the Dauphiné twin boundaries are not exactly parallel to the **a** axes, this model may be somewhat simplistic. In fact, Yamamoto et al. (1988) observe fringes at the boundary walls in their dark-field TEM micrographs, and they interpret these oscillations in intensity as arising from small displacements (less than 0.7 Å) in a direction that is nearly parallel to the twin boundaries.

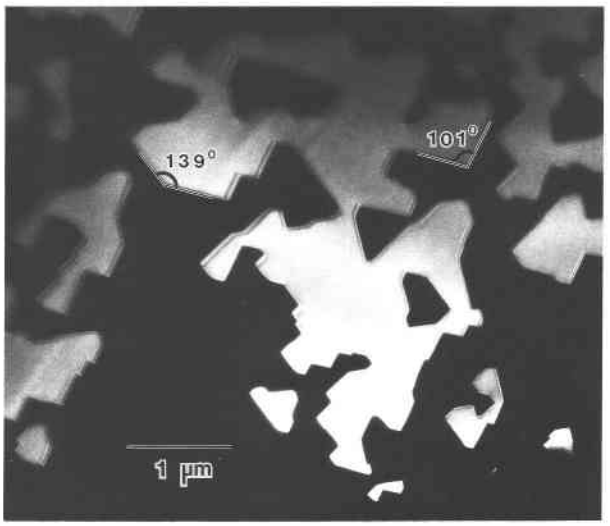


Fig. 3. A dark-field (**g** = 301) image of $\alpha$ quartz at room temperature. The two Dauphiné twin orientations appear as light and dark domains. These domains are polygonal, and boundary wall intersections are either 101° or 139°.

## The intermediate phase

### Early observations of anomalies at the critical temperature

When Le Chatelier first reported the phase transformation in quartz in 1889, he placed the inversion temperature at 570 °C. It now is known that the transition temperature decreases with increased impurity content (Keith and Tuttle, 1952; Ghiorso et al., 1979) and with smaller grain size (Dubrovinskiy and Piloyan, 1986), and the critical temperature commonly adopted today for pure macrocrystalline quartz is 573 °C. Optical studies of quartz revealed anomalous behavior at this transition point soon after Le Chatelier's discovery (see Sosman, 1965 for historical details), and one researcher (Steinwehr, 1938) actually concluded, from peculiarities in birefringence and rotatory polarization at the critical temperature, that quartz passes through two intermediate phases between the $\alpha$ and $\beta$ polymorphs.

This interpretation, however, was not widely believed, especially after Yakovlev et al. (1956) demonstrated that the transformation is accompanied by an intense scattering of light. Yakovlev et al. attributed this "critical opalescence" to fluctuations in the dielectric permeability, by analogy with the fluctuations in density that occur in liquid-gas mixtures as they transform to supercritical fluids. Shapiro and Cummins (1968) argued from Raman spectroscopic experiments that the source of this light scattering is static and not dynamic, but the explanation of Yakovlev et al. (1956) held a certain appeal because it seemed to offer an additional instance of the universality of critical phenomena.

Nevertheless, comprehensive examinations of the $\alpha$-$\beta$ quartz transition by diffraction techniques convincingly weigh against the onset of dielectric fluctuations at the critical temperature. In his seminal report of 1962, Young plotted the intensities of various X-ray diffraction spots against their twin equivalents [e.g., $I(301)$ vs. $I(30\bar{1})$] with increasing temperature, and two surprising observations came to light. First, primary extinction effects were severe in both the $\alpha$ and the $\beta$ phases, but, at the transition itself, extinction was strongly attenuated. Second, the crystal volume occupied by the two Dauphiné twin orientations became equal at the critical temperature, regardless of the original twin configuration. Young (1962) inferred from these results that as $\alpha$ quartz transforms to $\beta$ quartz, the macroscopic Dauphiné twin domains are replaced by fine-scale microtwins that subsequently disappear as the temperature is raised further. These microtwins explained not only the extinction relief and the equal twin volumes at the transition, but also the light scattering observed by Yakovlev et al. (1956).

### Imaging the Dauphiné microdomains

Proof of Young's (1962) hypothesis awaited real-space imaging of the $\alpha$-$\beta$ quartz transition, but the first photographs of the twin domains at the critical temperature were inconclusive. Inoue et al. (1974) examined square quartz plates that were 12 mm on a side and 0.3 mm thick via high-temperature X-ray transmission topography, and they failed to identify the microtwins postulated by Young (1962). With hindsight, it is clear that the "minute triangular or needle-like substructures" Inoue et al. (1974) observed in specimens cut normal to **a*** did in fact correspond to the microtwins, but the resolution of the technique (on the order of tens of micrometers) rendered the results ambiguous.

The limitations imposed by the poor resolution of X-ray topography were overcome by the use of a sample holder fitted with an internal furnace for the TEM. Van Tendeloo et al. (1976) and Malov and Sonyushkin (1976) were the first to observe the $\alpha$-$\beta$ quartz transition in situ

with the TEM, and both groups noted that as quartz is heated above the transition, the macroscopic Dauphiné twins disperse into a mosaic of triangular microtwins before transforming to $\beta$ quartz, thereby confirming Young's (1962) speculation.

Van Tendeloo et al. (1976) further revealed that the microtwins actually are triangular prisms elongate along the c-axis, and the twin walls can vibrate quite freely. Most remarkably, these triangular prisms become ordered into periodic arrays, with the size of the microtwins decreasing with increasing temperature (Fig. 4A). The continuity between arrays of unlike twin size is maintained through the insertion or deletion of rows of triangles (Fig. 4B), quite like dislocations but on a coarser scale. Similarly, point defects, consisting either of missing or additional triangles, also are commonly seen (Van Tendeloo et al., 1976), and theoretical analyses of these defect structures are offered by Snoeck et al. (1986) and Koh and Yamada (1987). As shown by Van Goethem et al. (1977), the microtwin mosaic will never interact with Brazil twin boundaries, which separate regions of opposite chirality. Brazil twin domains are joined by a distorted network of O atoms, the bonds of which would be broken by the tetrahedral rotations that relate the two Dauphiné twin orientations. Consequently, Dauphiné twins contained within a Brazil twin domain are isolated from and act independently of the surrounding microtwins in other Brazil twin domains.

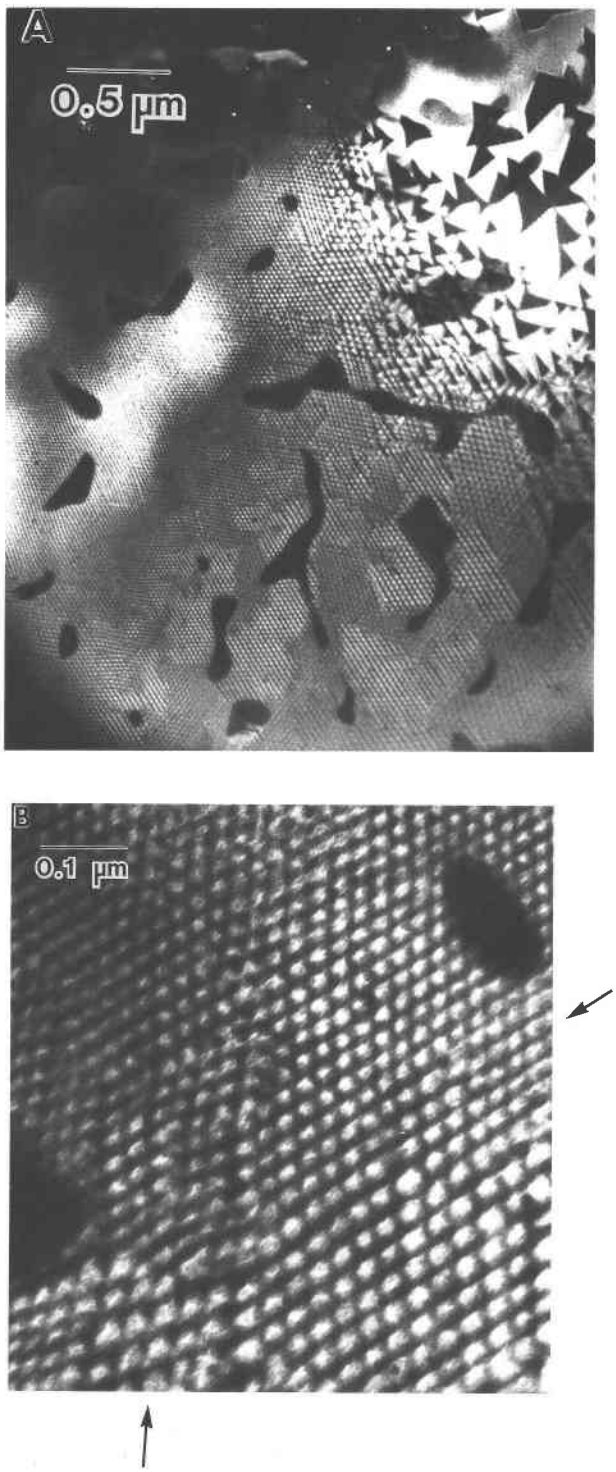


Fig. 4. (**A**) The intermediate phase of quartz. A temperature gradient exists across the specimen, with temperature increasing toward the lower left. Large Dauphiné twins can be seen to grade into triangular microtwins, which assemble into an ordered, honeycomb-like mosaic. Macrodomains appear as regions of differing contrast within the mosaic. Dark, irregularly shaped blobs are grains of Cu that were deposited on the specimen in an attempt to decrease thermal gradients. The c-axis is normal to the image. (**B**) An enlarged image of the incommensurate phase. By viewing the image along the arrows, dislocation-like features are clearly evident.

### Establishment of the microdomains as an incommensurate phase

With higher temperatures, the Dauphiné microtwins grow steadily less distinct, to the point at which they no longer can be imaged, and the specimen enters the $\beta$ stability field. Whether or not the passage of the microtwin arrays to $\beta$ quartz constitutes a discrete transition was not resolved by these early TEM studies, and thus it was unclear whether the microtwins qualify as a thermodynamically distinct phase.

However, the existence of a separate intermediate phase was predicted on theoretical grounds. Aslanian and Levanyuk (1979, 1984) and Aslanyan et al. (1983) proposed that a soft mode, created by tetrahedral oscillations between the two Dauphiné twin orientations, couples with an acoustic mode at the transition and thereby produces an incommensurate phase. The free energy of transition, as modeled by a Landau expansion, predicts that the transformation of the incommensurate phase to $\beta$ quartz is second order and that two types of incommensurate structures should be stable. One structure would manifest a periodicity in three directions, as do the ordered tri-

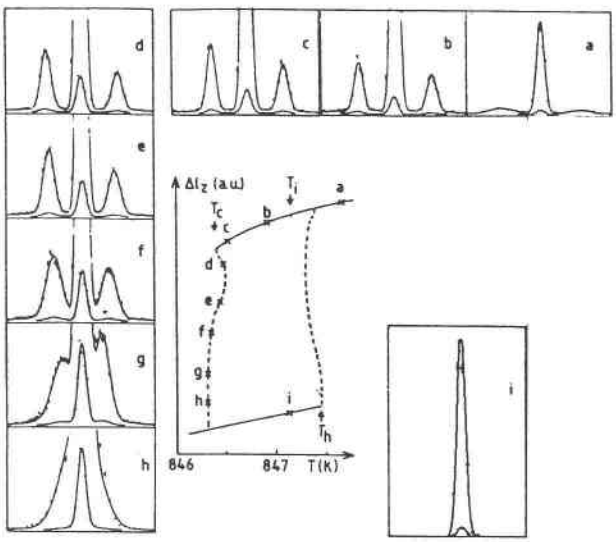


Fig. 5. The variation of the thermal expansion $\Delta l_z$ in arbitrary units reveals a thermal hysteresis at $T_c$ (central graph). The surrounding curves show the evolution of the satellites around the 030 spot with decreasing temperature, as determined by neutron diffraction. (From Dolino et al., 1984b.)

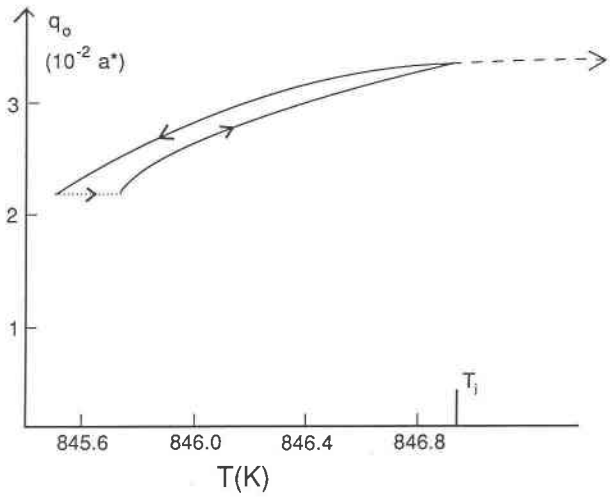


Fig. 6. Variation of the magnitude of the satellite wave vector $\mathbf{q}_o$ with temperature as revealed by $\gamma$-ray diffraction. Hysteresis between heating and cooling cycles again is observed. Electron diffraction results of the present study (dashed line) suggest that above $T_i$ the curves actually are asymptotic to $|\mathbf{q}_o| = 3.353 \times 10^{-2}$, which corresponds to a superperiodicity of approximately 30 Å. (After Bastie and Dolino, 1985.)

angular microtwins, and the other would be periodic in only one direction.

Experimental confirmation that an intermediate phase with a true field of stability exists between $\alpha$ and $\beta$ quartz was provided by Bachheimer (1980), who monitored changes in thermal expansion, elastic compliance, and birefringence simultaneously as specimens were heated above the transition temperature, $T_c$, at which $\alpha$ quartz transforms to the microdomain structure. Plots of each of these properties with increasing temperature reveal a slight change in slope approximately 1.3 °C above the critical temperature, suggesting the existence of a second-order transition at a higher temperature. Differential scanning calorimetry experiments by Zeyen et al. (1983) also indicate a discrete absorption event 1.3 °C above $T_c$, adding the first thermometric proof of a higher-temperature transition.

That the intermediate phase is incommensurate was demonstrated by Zeyen et al. (1983) as well as Dolino et al. (1984a, 1984b) via neutron scattering. In these studies, energy scans taken around the primary quartz diffraction spots detected distinct satellite intensities along the **a*** directions (Fig. 5). These satellite reflections occur as broad humps in diffraction patterns of $\beta$ quartz but sharpen into narrow intensities at $T_i$, the transition temperature between $\beta$ and the intermediate phase. The reciprocal space vector from the primary spot to the satellite spot, denoted as $\mathbf{q}_o$, decreases from 0.029 **a*** at $T_i$ to 0.015 **a*** at $T_c$. These reciprocal space lengths correspond to superperiodicities in real space that increase from approximately 150 Å at $T_i$ to approximately 288 Å at $T_c$. The continuous nature of the variation of $\mathbf{q}_o$ with temperature (Fig. 6) [as shown also by $\gamma$-ray diffraction (Bastie and Dolino, 1985)] substantiates the idea that the modulations in the intermediate phase are not commensurate with the primary quartz translations, as predicted by Aslanian and Levanyuk (1979).

## Reconciliation of diffraction results and images of the intermediate phase

The superperiodicities deduced from $|\mathbf{q}_o|$ in the neutron diffraction experiments are of the same magnitude as the spacings within the ordered array of Dauphiné microtwins as measured from the TEM images of Van Tendeloo et al. (1976). This coincidence led Zeyen et al. (1983) and Dolino et al. (1984a, 1984b) to identify the incommensurately modulated phase revealed by neutron diffraction with the microtwinned structure seen by electron microscopy. However, because careful X-ray transmission topography experiments by Zarka (1983) and Gouhara et al. (1983) could not resolve the ordered honeycomb mosaic visible in TEM micrographs, Gouhara and Kato (1985a) dismissed the microtwins as a "transient structure in an anomalous region near $T_c$." The triangular pattern, they asserted, is an artifact produced by the enormous strains attending large thermal gradients over extremely thin TEM specimens.

Nevertheless, Gouhara and Kato (1984) were able to detect satellite diffractions in their Laue photographs, and, like the satellites revealed by neutron scattering, these X-ray reflections denote a smooth change in modulation from 172 Å to 565 Å (Koh and Yamada, 1987). Gouhara

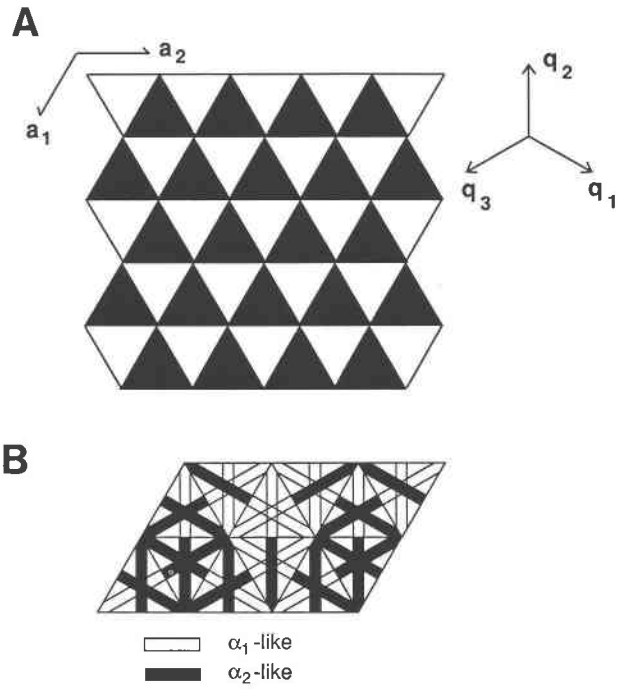


Fig. 7. (**A**) The microtwin model of Van Tendeloo et al. (1976). Dark triangles correspond to regions of one Dauphiné twin orientation, and white triangles represent areas of the other orientation. (**B**) The configuration wave model of Gouhara and Kato (1985a). Tetrahedral chains running along the $\mathbf{a}_1$, $\mathbf{a}_2$, and $\mathbf{a}_3$ directions oscillate between the $\alpha_1$ (black) and $\alpha_2$ (white) orientations, but trigonal symmetry is not obeyed. (From Gouhara and Kato, 1985a.)

and Kato (1985a, 1985b) allege that these satellites are produced not by microtwinned arrays but by "configuration waves." According to this model, the tetrahedral oscillations between the two Dauphiné twin orientations need not be correlated along $\mathbf{a}_1^*$, $\mathbf{a}_2^*$, and $\mathbf{a}_3^*$; within the large domains responsible for the superperiodicity, the structure may conform to the $\alpha_1$ orientation along one direction and to $\alpha_2$ along the other two directions (Fig. 7).

On a theoretical basis, this configuration wave model would appear to be problematic. The independence of the tetrahedral orientations among the $\mathbf{a}_1^*$, $\mathbf{a}_2^*$, and $\mathbf{a}_3^*$ directions violates the threefold rotational symmetry operation along **c**, raising the untenable idea that as trigonal $\alpha$ quartz transforms to hexagonal $\beta$ quartz, it passes through an intermediate phase with symmetry lower than either of the end-member phases. In addition, the microtwin model is supported by much circumstantial evidence. It was predicted by X-ray diffraction experiments (Young, 1962) before it was observed with the TEM. Further, as Van Landuyt et al. (1986) point out, the domain contrast in dark-field images of the intermediate phase is consistent with that expected for Dauphiné twins, and the $\alpha_1$ and $\alpha_2$ microdomains are related by twofold rotation, in accordance with group theoretical considerations.

However, evidence that the satellite reflections detected by neutron and X-ray diffraction are produced by an ordered array of microtwins could be provided only by selected area electron diffraction patterns of the microtwinned phase. Such satellites were obtained during high-temperature TEM experiments by Snoeck et al. (1986) and Heaney and Veblen (1987). Our study attempted specifically to correlate, at several distinct temperatures, the size of the Dauphiné microtwins with the periodicities indicated by satellite diffractions. Values for the supermodulation as determined by these separate methods consistently agreed to within 3%, which is less than the experimental measuring error. We believe that this concurrence provides convincing evidence that the microtwin arrays observed using electron microscopy constitute the intermediate phase of quartz.

### Electron diffraction of the intermediate phase

Like Snoeck et al. (1986), we recorded the evolution of the satellite spots with increasing temperature, and our observations closely parallel those obtained by other diffraction techniques (Fig. 8). At the critical temperature, $T_c$, we noted that the primary diffraction spots seemed sometimes to split slightly; this effect may have been a spurious one caused by warping of the specimen, but it is consistent with the two-peak structure observed at $T_c$ during the $\gamma$-ray diffraction experiments performed by Bastie and Dolino (1985). If genuine, this splitting would suggest that the lattices of the two Dauphiné twin orientations rotate slightly with respect to each other, perhaps to accommodate internal stresses produced at the onset of microtwinning.

Electron diffraction patterns obtained from the most coarsely microtwinned areas just above $T_c$ reveal diffuse intensities arranged along the $\pm\mathbf{a}_1^*$, $\mathbf{a}_2^*$, and $\mathbf{a}_3^*$ directions; in diffraction patterns corresponding to regions at slightly higher temperatures, the satellite spots move away from the primary spots and become much more distinct. The increase in the magnitude of the satellite vector $|\mathbf{q}_o|$ reflects the decrease in the size of the microtwins, whereas the sharpened satellite profile testifies to the rigorous order of the triangular prisms. When the temperature of the specimen is raised above $T_i$, however, the satellite spots become diffuse and only an astral streaking remains. It should be noted that it was never possible to excite all six satellite intensities simultaneously, probably because of the diffraction geometry of our experiments; rather, the specimens had to be rotated through an angle of approximately 1°, and films were double exposed to record the complete set.

We also observed the incommensurate phase with the electron beam parallel to several zone axes other than **c**—specifically, the [100], [210], [521], and [311] directions. Satellite spots could be seen in electron diffraction patterns corresponding to each of these zone axes, in some cases because the thin foils produced satellite rods rather than points. They always appeared on opposite sides of the primary spots along the $[hk0]^*$ directions. However,

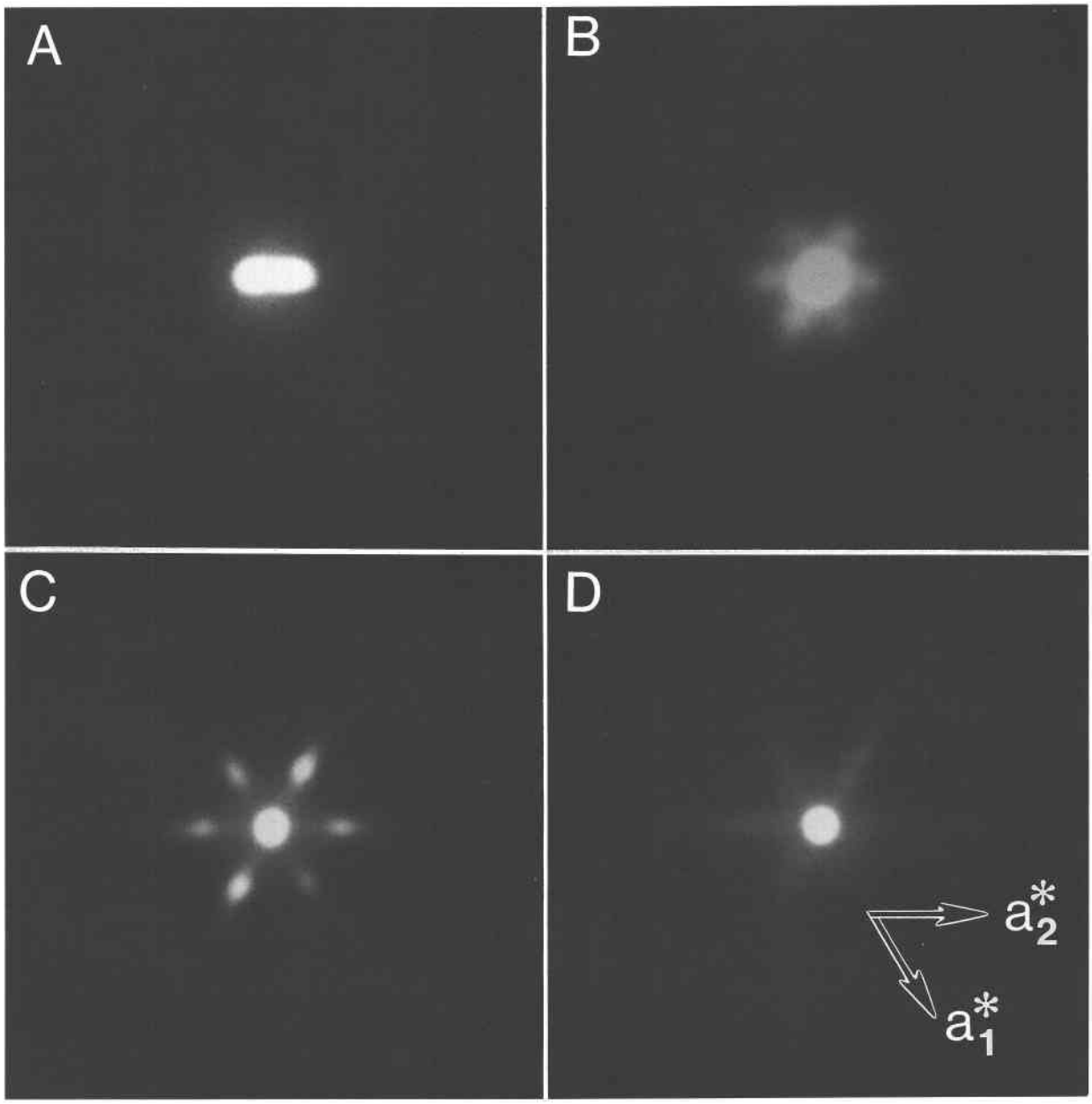


Fig. 8. Evolution of the 301 spot with temperature: **(A)** at $T_c$; **(B)** at $T_1 > T_c$; **(C)** at $T_2 > T_1$; **(D)** above $T_i$.

it appeared from diffraction patterns obtained with the beam parallel to [100] (Fig. 9) that the satellite vector $\mathbf{q}_o$ may not lie exactly within the (001) plane; rather, $\mathbf{q}_o$ contains a small but not negligible component along **c**. Although this result may have arisen from the diffraction geometry, this observation instead may indicate that the triangular prisms comprising the microtwins are actually tilted slightly away from the *c* axis, as was suggested by Yamamoto et al. (1988) on the basis of electron micrographs of the intermediate phase.

In reality, the satellite intensities were not always arranged with perfect sixfold symmetry around the primary spots because of systematic extinction effects (Fig. 10). A defect with displacement vector **b** normal to a reciprocal space vector **g** is not visible in dark-field images in which **g** is the operating beam (Hirsch et al., 1977); this relationship is known as the $\mathbf{g}\cdot\mathbf{b} = 0$ invisibility criterion. Likewise, displacements parallel to a given plane (*hkl*) will not appear in dark-field images when the beam $\mathbf{g}_{hkl}$ is imaged. As pointed out by Yamamoto et al. (1988), when $\mathbf{q}_o$ is parallel to **g**, dark-field images formed from **g** will fail to reveal the modulation fringes that are normal to $\mathbf{q}_o$, and, in diffraction patterns, the satellite intensities surrounding **g** will be systematically extinct along the $\mathbf{q}_o$ direction. Indeed, Dolino et al. (1984a) observed in their neutron diffraction patterns that (*h*00) reflections are sur-

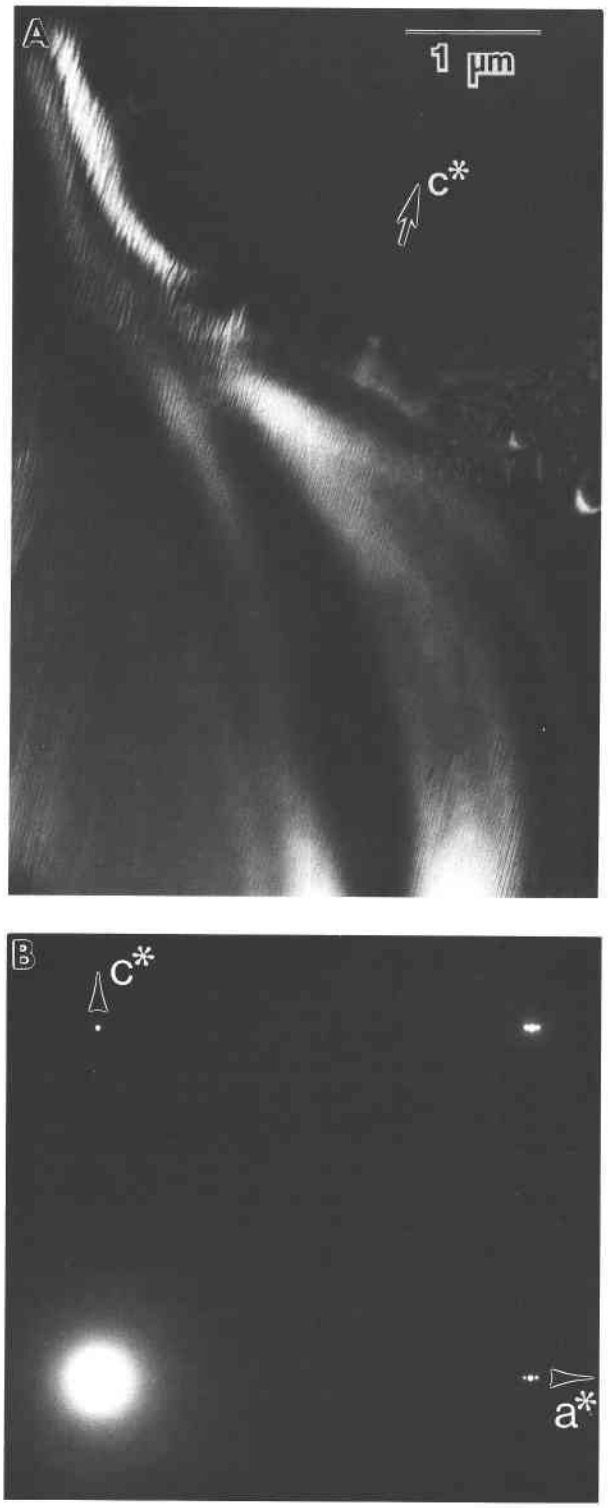


Fig. 9. (**A**) Dark-field (**g** = 301) image of incommensurate phase with $c$ in the plane of the image. Dauphiné microtwins appear as vertical black and white prisms. (**B**) SAED pattern of the incommensurate phase containing **a*** and **c***. Note that satellites appear to be displaced very slightly along **c***.

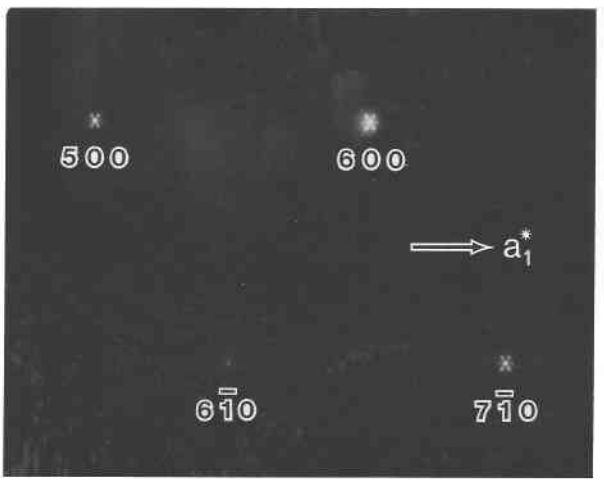


Fig. 10. Electron diffraction with the beam parallel to **c** reveals weaker satellite intensities along the **a*** direction due to extinction effects. Those intensities that can be seen along **a*** probably are caused by dynamical diffraction. Higher-order harmonics also are visible.

rounded by only four satellites; the satellites parallel to **a*** are absent.

### Macrodomains within the intermediate phase

X-ray topography experiments by Gouhara and Kato (1984) demonstrate that the satellite spots are actually split; within the $hk0$ reciprocal lattice plane, $\mathbf{q}_o$ deviates from **a*** by an angle of $\pm\varphi$, and this angle decreases with increasing temperature. Using a high-voltage TEM, Yamamoto et al. (1988) confirmed this satellite splitting with electron diffraction (Fig. 11) and they measured a decrease in $\varphi$ from 11° to 1° as the superperiodicity decreases from approximately 450 Å to 140 Å. These results suggest that the incommensurate phase consists of sets of macrodomains composed of microtwins of the same size but rotated by an angle of $2\varphi$ with respect to each other. The existence of such sets of macrodomains was predicted on a theoretical basis by Walker (1983), who modeled the free energy of the domain walls as a function of their orientations, and the configuration of these macrodomains was delineated on electron micrographs of the intermediate phase by Van Landuyt et al. (1985). Yamamoto et al. (1988) note that the value for $\varphi$ at $T_c$ (approximately 11°) is nearly the same as the value of the angle $\epsilon$ (the deviation between **a*** and the Dauphiné twin boundaries of $\alpha$ quartz) at $T_c$, suggesting a relationship between the two.

In our dark-field (**g** = 301) images of the incommensurate phase, such as Figure 4A, we noted that, within the two sets of macrodomains, the contrast among the constituent microtwins was distinctly different. Although the microtwins corresponding to one $\varphi$ orientation displayed extremely sharp intensity differences, the microtwins rotated in the opposite sense exhibited a less marked contrast. Consequently, in one set of macrodomains, the

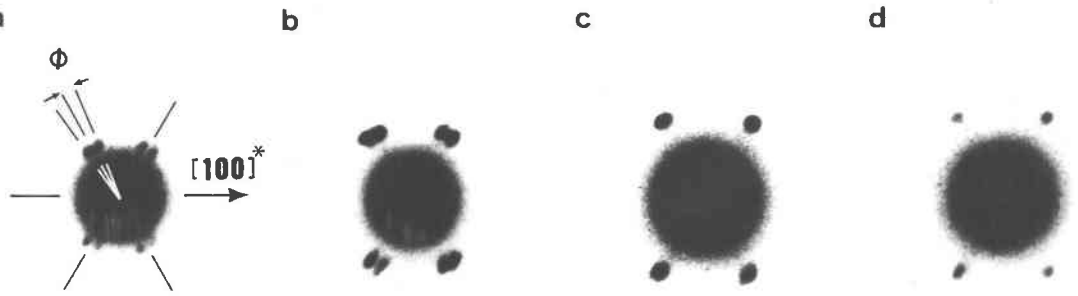


Fig. 11. The (100) spot surrounded by split satellite diffractions. This splitting is produced by the relative rotation of the two sets of macrodomains in the incommensurate phase. As temperature increases from (**a**) to (**d**), the angle $2\varphi$ of splitting decreases and the satellite pairs merge. (Reprinted from Yamamoto et al., 1988.)

Dauphiné mosaic is starkly black and white, whereas the other set of macrodomains appears more uniformly gray. This disparity in macrodomain intensities may arise from a rotation of macrodomain lattices relative to each other. As mentioned above, our electron diffraction work suggests that the microtwin prism axis is tilted slightly away from **c**; if the two macrodomains are not rotated from the **c**-axis in the same direction, then they will satisfy the Bragg diffraction conditions at different orientations. Thus, in a photograph taken at a single orientation, only one type of macrodomain will be in strong contrast.

This variation in intensity of macrodomains may explain a puzzling phenomenon observed in X-ray topography experiments. In dark-field images of quartz plates heated to approximately 0.1 °C above $T_c$, Gouhara and Kato (1985b) observed light and dark striations tens of micrometers in width (Fig. 12). These striations are not rigorously uniform in width, and they are elongate along **c**. Light scattering experiments by Dolino (1980) likewise indicate that cylinders with axes parallel to **c** that are tens of micrometers in diameter are associated with the intermediate phase of quartz. It is possible that these rod-like structures correspond to macrodomains.

Alternatively, the striations observed by Gouhara and Kato may be true Dauphiné microtwins. Although the largest microtwins observed by electron microscopy are only approximately 500 Å in width, $\gamma$-ray diffraction (Bastie and Dolino, 1985) has resolved satellite spacings that point to microtwins up to 850 Å wide. That larger individual microtwins have not been detected in electron images may be due to a genuine thin film effect. In crystals of sufficient size, Dauphiné microtwins may grade continuously from tens of micrometers to tens of ångströms over the 1.3 °C stability field of the incommensurate phase. Diffraction studies employing infrared radiation with a wavelength that approximates the cylinder diameters may help resolve this problem.

### Existence of a 3q to 1q transition

It also should be noted that some recent experimental work suggests that at a temperature just less than that of the transition to $\beta$ quartz, the incommensurate phase transforms to a structure that is modulated not along three directions but along only one. This transition from a **3q** to a **1q** state was predicted by Aslanian and Levanyuk (1979), and it had been observed in specimens exposed to a uniaxial stress in the (001) plane by elastic neutron scattering (Dolino et al., 1987) and by synchrotron X-ray diffraction (Zarka et al., 1988). However, a high-resolution neutron diffraction study by Bastie et al. (1988) in-

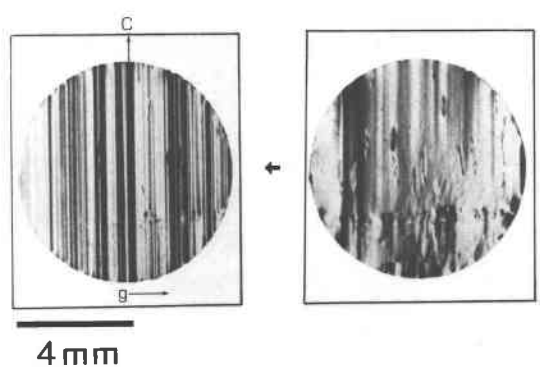


Fig. 12. Large-scale striations parallel to **c** emerge in X-ray topographs (**g** = 010) of quartz plates cooled from $T > T_c + 0.05$ °C (**right**) to $T < T_c + 0.05$ °C (**left**). (Reprinted from Gouhara and Kato, 1985b.)

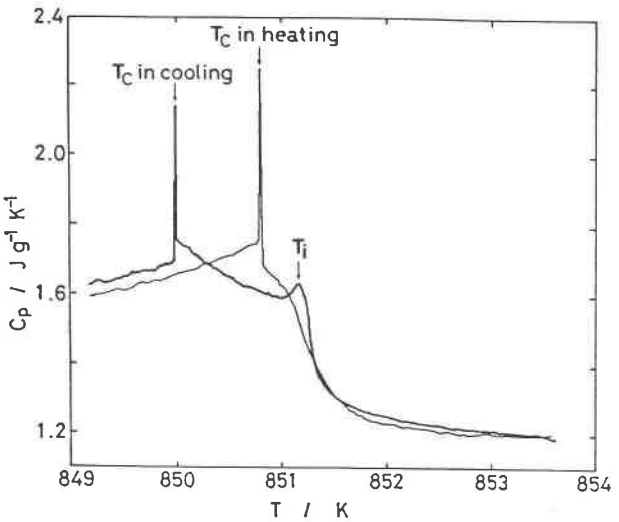


Fig. 13. The ac-calorimetry of quartz near the transition temperature clearly manifests the discrepancy between $T_c$ on cooling (thick curve) and $T_c$ on heating (thin curve), as is consistent with a first-order transition. (From Hatta et al., 1985.)

dicates that 3**q**-modulated crystals under no applied stress also may invert to a 1**q** state at 0.025 °C below the transition to $\beta$ quartz. Furthermore, the coexistence of the 3**q** satellite peaks with the 1**q** peak at the lower critical temperature suggests that the 3**q** to 1**q** transition is a first-order one. If such a transition actually occurs, it would appear that the transformation between $\alpha$ and $\beta$ quartz involves the temporary loss of trigonal symmetry; however, it also is possible that the appearance of a 1**q** state may be a response to internal stress associated with the intermediate phase.

## Thermodynamic order of the transition

The discovery of an intermediate phase between the $\alpha$ and $\beta$ quartz stability fields explains the difficulties that have plagued geochemists in their attempts to quantify changes in thermodynamic parameters at the transition. Certain irregularities attending this transformation have led some to describe it as a "quasi-first-order transition" (Helgeson et al., 1978), and others have asserted that "both first-order and second-order effects are present simultaneously" (Nordstrom and Munoz, 1985).

Even though thermodynamic parameters for the quartz transition can be modeled quite accurately using Pippard's relations for lambda transitions (Zeyen et al., 1983; Hosieni et al., 1985), enough evidence has been amassed to state with near certainty that the transition from $\alpha$ quartz to the incommensurate phase is in fact a first-order one. For example, clear hysteresis effects are observed by Shapiro and Cummins (1968) at the transition with regard to adiabatic elastic constants, as inferred from Raman and Brillouin scattering experiments. Likewise, Coe and Paterson (1969) investigated the $\alpha$-$\beta$ quartz transition in crystals under nonhydrostatic stress, and they note a hysteresis in $(\delta T/\delta\sigma)$ while cycling above and below $T_c$.

In his demonstration of the existence of the intermediate phase, Bachheimer (1980) detected hysteresis effects occurring simultaneously among thermal expansion coefficients, birefringence, and selected elastic constants. Differential scanning calorimetry by Zeyen et al. (1983) revealed discrepancies in $T_c$ depending upon the direction of approach to the transition, and a hysteresis in $T_c$ with respect to both temperature and pressure was demonstrated by the differential thermal analysis experiments of Raz (1983). As seen in Figure 13, the difference between $T_c$ on heating and $T_c$ on cooling is exceptionally clear in the ac calorimetry experiments performed by Hatta et al. (1985). Furthermore, both $\gamma$-ray (Bastie and Dolino, 1985) and neutron diffraction (Dolino et al., 1984b) revealed a hysteresis in the change in the length of the satellite vector $\mathbf{q}_0$ with temperature. Dolino et al. (1984b) also observed the coexistence of $\alpha$-quartz with the intermediate phase. All of these results imply that genuine discontinuities exist in the enthalpy, entropy, and volume of transition, and the finite values for $\Delta V$ and $\Delta H$ reported by Ghiorso et al. (1979) support this interpretation.

## The structure of $\beta$ quartz

In dark-field images of the incommensurate phase of quartz, the microtwins grow less and less distinct with increasing temperature, and eventually they cannot be distinguished at all. The diminishing size of the microtwins with higher temperature is partly responsible for this loss of detail, and this effect is exacerbated by the comparatively poor resolution of the electron microscope in the dark-field mode. Nevertheless this deterioration in contrast also reflects a genuine change in the nature of the quartz structure as the temperature increases.

On the basis of Young's X-ray study in 1962, Höchli and Scott (1971) computed a gradual decrease in the tetrahedral rotation angle $\theta$ from 16° at room temperature to 7° at the onset of the transition. As the twin domains grow structurally more alike, the disparity in the intensities of the (301) and the (30$\bar{1}$) diffractions decreases slightly, as was observed by Young (1962). Accordingly, the contrast between the two twin orientations might be expected to decrease in dark-field images in which (301) is the imaging beam.

Furthermore, a plot of the variation in the tetrahedral tilt angle $\theta$ against distance along any direction normal to **c** would resemble a block wave; most of the tetrahedra occupy one of the two Dauphiné twin orientations (Liebau and Böhm, 1982). Only at the narrow boundaries do they depart appreciably from angles of $\pm 7°$. As the microtwins grow smaller, however, the block wave gradually transforms into a sinusoidal wave, since fewer and fewer of the tetrahedra are tilted to their extremes. Consequently, the intermediate phase evolves from a domain-dominated structure to a boundary-dominated one,

and the dark-field contrast between the two Dauphiné microtwin orientations becomes dramatically weaker.

Therefore, the TEM images of the incommensurate phase near $T_i$ are inherently indistinct and cannot by themselves answer a question they immediately provoke: What is the structure of $\beta$ quartz? Do the microtwins steadily decrease in size until they approach the scale of the unit cell? If so, are these unit-cell-sized twins static or dynamic? Or conversely, does the ideal hexagonal $\beta$ quartz configuration at the boundary of the microtwins continue to grow at the expense of the trigonal microtwins with higher temperature, such that the space group of $\beta$ quartz truly conforms to $P6_222$?

## Experimental attempts to determine the $\beta$-quartz structure

**Previous work.** If $\beta$ quartz exists as a static structure with true hexagonal symmetry, each atom should be restricted to a single equilibrium potential well, whereas the atoms in a dynamic structure would oscillate rapidly between two separate potential minima. Differentiation between these two models by conventional diffraction methods requires two separate least squares refinements—one of a structure in which each site is occupied by a whole atom and another of a structure in which twice as many sites are occupied by half atoms. The model that yields the better agreement with observed diffraction data should correspond to the true structure. X-rays, however, are not sufficiently sensitive to these subtle structural deviations to settle the question decisively, and early efforts using this approach (e.g., Arnold, 1965) were unconvincing.

In order to circumvent this problem, Young (1962) defined and measured a parameter $Q$—the ratio of the magnitudes of a given structure factor in the high-temperature and low-temperature phases. Young developed a theoretical model to predict values for $Q$ based on a two-potential $\beta$ phase, but he extrapolated from experimental data to predict $Q$ values for a static $\beta$ structure. Perhaps not surprisingly, the observed values of $Q$ correlate more closely with those ratios derived from the extrapolated data than from the theoretical model, and Young concluded that a single-minimum structure best fits the observed results. Consequently, Young averred that $\beta$ quartz is a static structure with true hexagonal symmetry, even on a local scale.

Young also observed that the mean-square displacements of the atomic thermal ellipsoids increase significantly along all directions near the transition temperature, and that the axes of the ellipsoids are rotated away from their idealized orientations. For instance, at 580 °C the direction of maximum vibration for O atoms is rotated by 21° from the normal to the Si-O-Si plane in the idealized hexagonal structure. Young attributed these anomalies to anharmonic vibration, and a recent single crystal X-ray study of quartz by Kihara (1990) attempted to account for the anharmonic character of the thermal vibrations in quartz by introducing higher order terms into the structure factor expression.

Kihara examined in detail the changes in the dimensions and orientations of the O and Si thermal ellipsoids with increasing temperature, and he argued that his experiments confirm the single-minimum model proposed by Young. In particular, Kihara noted that the error value obtained from a split-atom refinement ($R_{SP}$ = 2.76%) is higher than that produced by a single-atom refinement ($R_{4G}$ = 2.44%) at 575 °C. Kihara also asserted that the probability density function for the O atom in $\beta$ quartz is unimodal, and he observed that the primary axis of the O thermal ellipsoid is tilted slightly away from the line joining the presumed $\alpha_1$ and $\alpha_2$ O atom positions.

Nevertheless, it would seem that Kihara's (1990) data offer equally strong support for a double-minimum model for $\beta$ quartz. As Kihara pointed out, the thermal ellipsoid for O in $\beta$ quartz is highly anisotropic, with the mean-square displacement along the primary axis attaining values between 0.09 and 0.10 Å$^2$. While it may be true that this primary axis does not coincide exactly with the $\alpha_1$-$\alpha_2$ join between O atom positions, it seems more remarkable that as quartz is heated from room temperature to 575 °C, the primary axis rotates from more than 45° away from the join to within 3° of the $\alpha_1$-$\alpha_2$ join. In addition, the probability density function for O in $\beta$ quartz deviates dramatically from a Gaussian distribution and displays a weak but distinct bimodality, even when refined from the single-minimum model. Lastly, the lower error value achieved for the single-minimum structure appears less persuasive when one considers that the split-atom refinement was performed without the benefit of the higher-order terms in the structure factor expression; therefore, the split-atom refinement was computed using only 16 variables, whereas the single-minimum refinement contained 23 variables.

Other researchers who have studied the structure of $\beta$ quartz using techniques other than X-ray diffraction have tended to support the double-mininum model. For instance, Wright and Lehmann (1981) performed neutron diffraction refinements of powdered and single crystals of $\beta$ quartz at 590 °C using the Rietveld technique, and they found that when split O atoms are refined in the general position, error values are markedly smaller than when single atoms are located in special positions ($R_{general}$ = 3.8% while $R_{special}$ = 5.3%). Optimal refinement was obtained when equivalent O atoms in the Dauphiné twinned positions were separated by 0.4 Å, which corresponds to a tetrahedral rotation angle of approximately 5.7°. Si atoms, on the other hand, refined near their ideal hexagonal positions. Although diffraction experiments cannot distinguish between a dynamic structure and a static structure with microtwins at the scale of the unit cell, Wright and Lehmann proposed that $\beta$ quartz is a dynamic structure characterized by correlated, low-frequency tetrahedral oscillations.

Spectroscopic studies also seem to support this interpretation. The discovery that certain phase transitions are

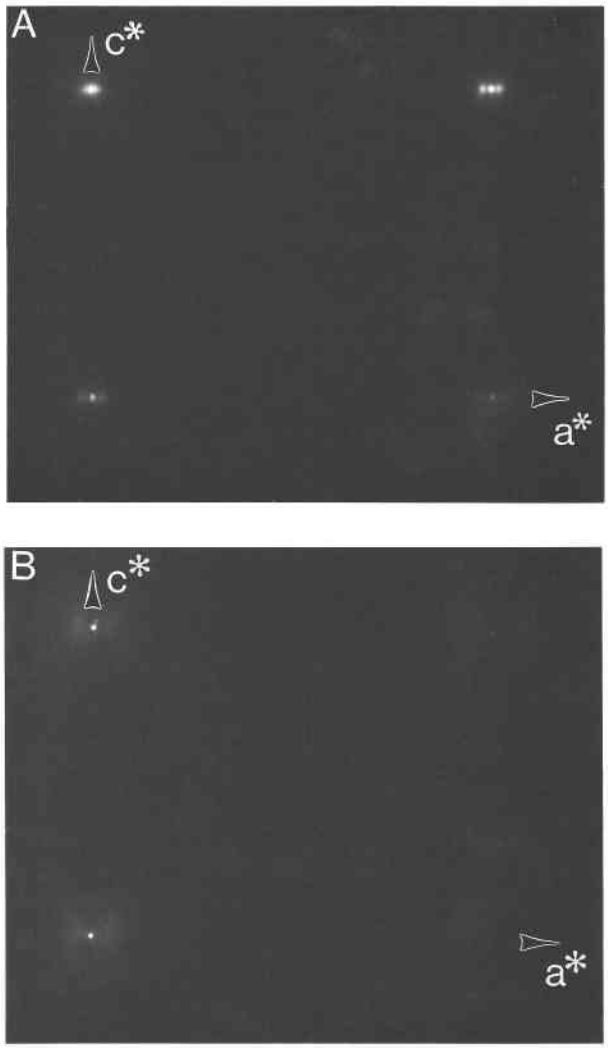


Fig. 14. Satellite intensities persist above the transition to $\beta$ quartz as diffuse ellipsoids elongate along **c**. (**A**) $T_i$ + 10 °C; (**B**) $T_i$ + 200 °C.

marked by the disappearance of specific vibrational modes—denoted as soft modes—was made by C. V. Raman during an investigation of the $\alpha$-$\beta$ quartz transition (Raman and Nedungadi, 1940). This mode occurs at 207 $cm^{-1}$, and Kleinman and Spitzer (1962) attributed it to movement of O atoms perpendicular to the Si-O-Si plane; this motion corresponds to that of O atoms as quartz tetrahedra rotate from one Dauphiné twin orientation to the other.

Subsequent neutron scattering experiments have indicated that this mode does not vanish entirely at the transition temperature. Inelastic neutron scattering (Axe and Shirane, 1970) revealed that even at $T_i$ + 214 °C, weak critical inelastic scattering underlies the primary Bragg peaks; Axe and Shirane interpreted these weak intensities as evidence for overdamping of the soft mode. Dolino et al. (1984a, 1984b) observed that the satellite intensities produced by neutron diffraction in the incommensurate phase persist as extremely weak intensities 2 °C above the transition to $\beta$ quartz, and they explained this phenomenon in terms of the overdamped soft mode proposed by Axe and Shirane.

**This work.** Our **c**-axis electron diffraction patterns of $\beta$ quartz also manifested a faint streaking along the six [100]* directions; however, since these streaks coincided with those expected from thermal diffuse scattering (TDS), specimens also were examined along zone axes perpendicular to **c**. These diffraction patterns showed that the satellites are elongate parallel to **c*** and that they definitely are present at temperatures well over $T_i$; diffuse satellite intensities were observed 200 °C above the transition temperature (Fig. 14).

To test the hypothesis that this phenomenon is an expression of thermal diffuse scattering, a series of diffraction patterns were recorded from the same area at successively higher temperatures. Care was taken to maintain the same primary beam intensity and exposure times throughout. The satellite intensities grew gradually fainter with higher temperature, although they never disappeared. This behavior is contrary to that expected for diffracted intensity resulting from TDS; in fact, some diffuse streaks that were not associated with the satellites grew increasingly intense with temperature, and it is assumed that these did arise from TDS. On cooling the specimens back toward the transition temperature, the satellites reversibly regained their original intensities. Thus, the decreased intensity of the satellites with higher temperature was not caused by electron beam damage.

Although the satellites decreased in intensity and sharpness with increasing temperature above $T_i$, they did not move perceptibly away from the primary Bragg spots. Consequently, $|\mathbf{q}_o|$ appears to be constant above $T_i$, and plots of $|\mathbf{q}_o|$ vs. temperature seem to be asymptotic (Fig. 6). The diffuseness and elongation of the satellite spots observed in electron diffraction patterns suggest that the satellites are of inelastic origin, but their continuous behavior through $T_i$ suggests that some kind of local structural correlation is sustained into the $\beta$ phase. The structure of $\beta$ quartz that emerges from these results is one in which the tetrahedra oscillate between two equilibrium positions but are ordered over short ranges. Such coherency among tetrahedral fluctuations over the small scale is, perhaps, to be expected; Si-O-Si linkages must limit significantly the degree of randomness attainable in the movement between nearest-neighbor tetrahedra.

## Conclusions

Although the phase transformation between $\alpha$ and $\beta$ quartz traditionally has been regarded as a simple, second-order transition, experiments employing visible light, X-rays, electrons, neutrons, and $\gamma$-rays have revealed its true complexity. It now appears that $\alpha$ quartz undergoes a first-order transformation to an incommensurate intermediate phase that is stable over a 1.3 °C temperature interval. The superperiodicities that characterize this phase arise from the ordering of triangular Dauphiné mi-

crotwin prisms elongate along **c**, and the modulation of this intermediate phase decreases continuously with increasing temperature. The transition from the intermediate phase to $\beta$ quartz has been difficult to characterize through imaging techniques, but calorimetry suggests that it is second order.

Results from both diffraction and spectroscopy experiments indicate that the structure of $\beta$ quartz is dynamic. Researchers who have studied $\beta$ quartz using single crystal X-ray diffraction methods favor a model in which each Si and O atom is characterized by high thermal vibration but occupies a single potential minimum (Young, 1962; Kihara, 1990). Nevertheless, on the basis of our own electron diffraction experiments and the work of others (e.g., Boysen et al., 1980; Wright and Lehmann, 1981; Dolino et al., 1983), we support a model in which at least the O atoms librate between two potential minima separated by an extremely small potential maximum. We suggest that the silica tetrahedra oscillate rapidly between the two orientations corresponding to the Dauphiné twins, and that over short ranges the tetrahedral rotations are temporally correlated.

Consequently, the $\alpha$ to $\beta$ quartz transition may in some sense be akin to ferromagnetic transitions at the Curie point. Above $T_i$, tetrahedra oscillate between the two Dauphiné twin positions without long-range correlations, but, as $T_i$ is approached, the correlation distance steadily increases. Tetrahedral lock-in is complicated by the coupling of the oscillatory mode with a transverse acoustic mode at $T_i$, thereby producing an incommensurate phase, but, at $T_c$, lock-in occurs. Thus, despite the complexity of the $\alpha$-$\beta$ quartz transition, it has been accurately modeled by the Landau theory of first-order transitions (Höchli and Scott, 1971; Grimm and Dorner, 1975; Aslanian and Levanyuk, 1979). A similar approach has been proposed for the $P\bar{1}$ to $I\bar{1}$ transition in anorthite (Ghose et al., 1988), suggesting that displacive phase transitions in many mineral systems may be interpreted as structural order-disorder events.

## Acknowledgments

We would like to thank Charlie Burnham and Jim Thompson for inspiring our interest in phase transitions in minerals. In addition, we are grateful to Gordon Nord and to Charlie Burnham for their first-order reviews of this manuscript. We also would like to express our appreciation to Pete Dunn and Jeff Post at the U.S. National Museum for supplying the specimen used in this study. Helpful discussions were provided by Jeff Post, George Guthrie, and Eugene Smelik. Original photographs reproduced in this paper were very kindly provided by Naoki Yamamoto and Kazutoshi Gouhara. Figures were reprinted from articles by J. Papike, H. Grimm, G. Dolino, P. Bastie, K. Gouhara, N. Yamamoto, and I. Hatta. Figure 5 is reprinted with the permission of Journal de Physique; figure 13 is reprinted with the permission of Elsevier. This research was supported by NSF grants EAR86-09277 and EAR89-03630. Electron microscopy was performed in the Johns Hopkins HRTEM laboratory, which was established with partial support from NSF grant EAR83-00365.

## References cited

Arnold, H. (1965) Diffuse röntgenbeugung und kooperation bei der $\alpha$-$\beta$-umwandlung von quartz. Zeitschrift für Kristallographie, 121, 145–157.

Aslanian, T.A., and Levanyuk, A.P. (1979) On the possibility of the incommensurate phase near $\alpha$-$\beta$ transition point in quartz. Solid State Communication, 31, 547–550.

——— (1984) Fluctuation effects as a cause for the incommensurate phase formation. Ferroelectrics, 53, 231–234.

Aslanyan, T.A., Levanyuk, A.P., Vallade, M., and Lajzerowicz, J. (1983) Various possibilities for formation of incommensurate superstructure near the $\alpha$-$\beta$ transition in quartz. Journal of Physics C, 16, 6705–6712.

Axe, J.D., and Shirane, G. (1970) Study of the $\alpha$-$\beta$ quartz phase transformation of inelastic neutron scattering. Physical Review B, 1, 342–348.

Bachheimer, J.P. (1980) An anomaly in the $\beta$ phase near the $\alpha$-$\beta$ transition of quartz. Journal de Physique—Lettres, 41, L559–L561.

Bastie, P., and Dolino, G. (1985) $\gamma$-ray-diffraction of an incommensurate phase: Application to quartz. Physical Review B, 31, 2857–2861.

Bastie, P., Mogeon, F., and Zeyen, C.M.E. (1988) Direct neutron observation of a single-**q** incommensurate phase of quartz at zero stress. Physical Review B, 38, 786–788.

Bates, F.J., and Phelps, F.P. (1927) A suggested new base point on the thermometric scale and the $\alpha$-$\beta$ inversion of quartz. National Bureau of Standards, Scientific Paper no. 557, 315–327.

Berge, B., Dolino, G., and Vallade, M. (1984) Incommensurate phase of quartz. II: Brillouin scattering studies. Journal de Physique, 45, 715–724.

Boysen, H., Dorner, B., Frye, F., and Grimm, H. (1980) Dynamic structure determination for two interacting modes at the M-point in $\alpha$- and $\beta$-quartz by inelastic neutron scattering. Journal of Physics C, 13, 6127–6146.

Bragg, W.H., and Gibbs, R.E. (1925) The structure of $\alpha$ and $\beta$ quartz. Proceedings of the Royal Society of London, A109, 405–427.

Buerger, M.J. (1951) Crystallographic aspects of phase transformations. In R. Smoluchowski, Ed., Phase transformations in solids, p. 183–211. Wiley, New York.

Coe, R.S., and Paterson, M.S. (1969) The $\alpha$-$\beta$ inversion in quartz: A coherent phase transition under nonhydrostatic stress. Journal of Geophysical Research, 74, 4921–4948.

Dolino, G. (1980) Angular and polarization properties of light scattering at the $\alpha$-$\beta$ phase transition of quartz. Physica Status Solidi, 60, 391–401.

——— (1990) The $\alpha$-inc-$\beta$ transitions of quartz: A century of research on displacive phase transitions. Phase Transitions, 21, 59–72.

Dolino, G., Bachheimer, J.-P., Gervais, F., and Wright, A.F. (1983) La transition $\alpha$-$\beta$ du quartz: Le point sur quelques problèmes actuels: Transition ordre-désordre ou displacive, comportement thermodynamique. Bulletin de Minéralogie, 106, 267–285.

Dolino, G., Bachheimer, J.P., Berge, B., and Zeyen, C.M.E. (1984a) Incommensurate phase of quartz: I. Elastic neuron scattering. Journal de Physique, 45, 361–371.

Dolino, G., Bachheimer, J.P., Berge, B., Zeyen, C.M.E., Van Tendeloo, G., Van Landuyt, J., and Amelinckx, S. (1984b) Incommensurate phase of quartz: III. Study of the coexistence state between the incommensurate and the $\alpha$-phases of neutron scattering and electron microscopy. Journal de Physique, 45, 901–912.

Dolino, G., Bastie, P., Berge, B., Vallade, M., Bethke, J., Regnault, L.P., and Zeyen, C.M.E. (1987) Stress-induced "3-q"–"1-q" incommensurate phase transition in quartz. Europhysics Letters, 3, 601–609.

Dubrovinskiy, L.S., and Piloyan, G.D. (1986) Effect of (micro) crystal size on the temperature of the polymorphic $\alpha$-$\beta$ transition in quartz. Doklady Adademii Nauk SSSR, 286, 958–961.

Ghiorso, M.S., Carmichael, I.S.E., and Moret, L.K. (1979) Inverted high-temperature quartz. Contributions to Mineralogy and Petrology, 68, 307–323.

Ghose, S., Van Tendeloo, G., and Amelinckx, S. (1988) Dynamics of a second-order phase transition: $P\bar{1}$ to $I\bar{1}$ phase transition in anorthite, $CaAl_2Si_2O_8$. Science, 242, 1539–1541.

Gibbs, R.E. (1925) The variation with temperature of the intensity of reflection of X-rays from quartz and its bearing on the crystal structure. Proceedings of the Royal Society of London, A107, 561–570.

Gouhara, K., and Kato, N. (1984) Refined observations of satellite reflections in the intermediate phase of quartz. Journal of the Physical Society of Japan, 53, 2177–2180.

——— (1985a) The intermediate phase of quartz. I. Journal of the Physical Society of Japan, 54, 1868–1881.

——— (1985b) The intermediate phase of quartz. II. Behaviour near the first-order transition temperature. Journal of the Physical Society of Japan, 54, 1882–1889.

Gouhara, K., Hao Li, Y., and Kato, N. (1983) Studies on the $\alpha$-$\beta$ transition of quartz by means of in situ X-ray topography. Journal of the Physical Society of Japan, 52, 3821–3828.

Grimm, H., and Dorner, B. (1975) On the mechanism of the $\alpha$-$\beta$ phase transformation of quartz. Physics and Chemistry of Solids, 36, 407–413.

Hatta, I., Matsuura, M., Yao, H., Gouhara, K., and Kato, N. (1985) True behavior of heat capacity in $\alpha$, incommensurate, and $\beta$ phases of quartz. Thermochimica Acta, 88, 143–148.

Heaney, P.J., and Veblen, D.R. (1987) Satellite reflections and memory effects observed by electron microscopy of the intermediate phase of quartz. Eos, 68, 433.

Helgeson, H.C., Delany, J.M., Nesbitt, H.W. and Bird, D.K. (1978) Summary and critique of the thermodynamic properties of rock-forming minerals. American Journal of Science, 278-A, 1–229.

Hirsch, P., Howie, A., Nicholson, R.B., Pashley, D.W., and Whelan, M.J. (1977) Electron microscopy of thin crystals, 563 p. Robert Krieger, Malabar, Florida.

Höchli, U.T., and Scott, J.F. (1971) Displacement parameter, soft-mode frequency, and fluctuations in quartz below its $\alpha$-$\beta$ phase transition. Physical Review Letters, 26, 1627–1629.

Hosieni, K.R., Howald, R.A., and Scanlon, M.W. (1985) Thermodynamics of the lambda transition and the equation of state of quartz. American Mineralogist, 70, 782–793.

Inoue, N., Iida, A., and Kohra, K. (1974) X-ray topographic investigation on phase transition in quartz. I. Experimental observations. Journal of the Physical Society of Japan, 37, 742–750.

Keith, M.L., and Tuttle, O.F. (1952) Significance of variance in high-low inversion of quartz. American Journal of Science, 253a, 203–280.

Kihara, K. (1990) An X-ray study of the temperature dependence of the quartz structure. European Journal of Mineralogy, 2, 63–77.

Kleinman, D.A., and Spitzer, W.G. (1962) Theory of the optical properties of quartz in the infrared. Physics Review, 125, 16–30.

Koh, S.-I., and Yamada, Y. (1987) Kinetic process of formation of discommensuration pattern in $SiO_2$. Phase Transitions, 8, 261–272.

Krishnamurti, D. (1958) The Raman spectrum of quartz and its interpretation. Proceedings of the Indian Academy of Science, A47, 276–291.

Lang, A.R. (1965) Mapping Dauphiné and Brazil twins in quartz by X-ray topography. Applied Physics Letters, 7, 168–170.

Le Chatelier, H. (1889) Sur la dilatation du quartz. Comptes Rendus de l'Académie des Sciences, 108, 1046–1049.

Liebau, F., and Böhm, H. (1982) On the co-existence of structurally different regions in the low-high quartz and other displacive phase transformations. Acta Crystallographica, A38, 252–256.

Malov, Y.V., and Sonyushkin, V.E. (1976) Direct electron-microscopic investigation of the $\alpha$-$\beta$ transition process in quartz. Soviet Physics Crystallography, 20, 644–645.

McLaren, A.C., and Phakey, P.P. (1969) Diffraction contrast from Dauphiné twin boundaries in quartz. Physica Status Solidi, 31, 723–737.

Megaw, H.D. (1973) Crystal structures: A working approach, 563 p. W.B. Saunders Company, Philadelphia.

Nordstrom, D.K., and Munoz, J.L. (1985) Geochemical thermodynamics, 477 p. Benjamin/Cummings, Menlo Park, California.

Papike, J.J. (1988) Chemistry of the rock-forming silicates: Multiple-chain, sheet, and framework structures. Reviews of Geophysics, 26, 407–444.

Parrish, W., and Gordon, S.G. (1945) Orientation techniques for the manufacture of quartz oscillator-plates. American Mineralogist, 30, 296–325.

Perrier, A., and Roux, H. (1923) Sur la possibilité de la calorimétrie adiabatique par voie électrique aux températures élevées et son application au quartz cristallisé. Mémoires de la Société vaudoise des Sciences naturelles, 1, 109–136.

Raman, C.V., and Nedungadi, T.M.R. (1940) The $\alpha$-$\beta$ transformation of quartz. Nature, 145, 147.

Raz, U. (1983) Thermal and volumetric measurements on quartz and other substances at pressures up to 6 kbars and temperatures up to 700 °C. Ph.D. dissertation, Swiss Federal Institute of Technology, Zurich.

Saksena, B.D., and Narain, H. (1949) Raman and infra-red spectra of quartz. Nature, 164, 583–584.

Shapiro, S.M., and Cummins, H.Z. (1968) Critical opalescence in quartz. Physical Review Letters, 21, 1578–1582.

Shigenari, T., and Shionoya, T. (1985) Light scattering studies on the intermediate phase near the $\alpha$-$\beta$ transition of quartz. Japanese Journal of Applied Physics, Supplement 24-2, 24, 162–165.

Snoeck, E., Roucau, C., and Saint-Grégoire, P. (1986) Electron microscopy study of the modulated phases in berlinite $AlPO_4$ and quartz. Journal de Physique, 47, 2041–2053.

Sosman, R.B. (1965) The phases of silica. Rutgers University Press, New Brunswick, New Jersey.

Steinwehr, H.E. (1938) Umwandlung $\alpha$-$\beta$-quartz. Zeitschrift für Kristallographie, 99, 292–313.

Van Goethem, L., Van Landuyt, J., Amelinckx, S. (1977) The $\alpha$-$\beta$ transition in amethyst quartz as studied by electron microscopy and diffraction. Physica Status Solidi, 41, 129–137.

Van Landuyt, J., Van Tendeloo, G., Amelinckx, S., and Walker, M.B. (1985) Interpretation of Dauphiné-twin-domain configurations resulting from the $\alpha$-$\beta$ phase transition in quartz and aluminum phosphate. Physical Review B, 31, 2986–2992.

Van Landuyt, J., Van Tendeloo, G., and Amelinckx, S. (1986) Reply to "Intermediate phase between the $\alpha$ and $\beta$ phases of quartz." Physical Review B, 34, 2004–2006.

Van Tendeloo, G., Van Landuyt, J., and Amelinckx, S. (1976) The $\alpha$-$\beta$ phase transition in quartz and $AlPO_4$ as studied by electron microscopy and diffraction. Physica Status Solidi, 33, 723–735.

Walker, M.B. (1983) Theory of domain structures and associated defects in the incommensurate phase of quartz. Physical Review B, 28, 6407–6410.

Walker, M.B., and Gooding, R.J. (1985) Properties of Dauphiné-twin domain walls in quartz and berlinite. Physical Review B, 32, 7408–7411.

Wright, A.F., and Lehmann, M.S. (1981) The structure of quartz at 25 and 590 °C determined by neutron diffraction. Journal of Solid State Chemistry, 36, 371–380.

Yakovlev, I.A., Mikheeva, L.F., and Velichkina, T.S. (1956) The molecular scattering of light and the $\alpha$-$\beta$ transformation in quartz. Soviet Physics—Crystallography, 1, 91–98.

Yamamoto, N., Tsuda, K., and Yagi, K. (1988) High voltage electron microscope study of incommensurate phase in quartz. Journal of the Physical Society of Japan, 57, 1352–1364.

Young, R.A. (1962) Mechanism of the phase transition in quartz. U.S. Air Force, Office of Scientific Research, Contract No. AF 49(638)-624.

Zarka, A. (1983) Observations on the phase transition in quartz by synchrotron-radiation X-ray topography. Journal of Applied Crystallography, 16, 354–356.

Zarka, A., Capelle, B., and Petit, M. (1988) Evidence of a single-**q** incommensurate phase in quartz by synchroton X-ray diffraction. Journal of Applied Crystallography, 21, 72–73.

Zeyen, C.M.E., Dolino, G., and Bachheimer, J.P. (1983) Neutron and calorimetric observation of a modulated structure in quartz just above the $\alpha$-$\beta$ phase transition. Physica, 120B, 280–282.

Manuscript received February 3, 1990
Manuscript accepted February 15, 1991